

## Structural control in self-standing mesostructured silica oriented membranes and xerogels†

G. J. A. A. Soler-Illia,<sup>a</sup> E. L. Crepaldi,<sup>a</sup> D. Grosso,<sup>a</sup> D. Durand<sup>b</sup> and C. Sanchez<sup>z\*</sup>

<sup>a</sup> Laboratoire de Chimie de la Matière Condensée UMR 7574, Université Pierre et Marie Curie, 4 Place Jussieu, 75252 Paris Cedex 05, France. E-mail: clems@ccr.jussieu.fr

<sup>b</sup> LURE Bât 209D Centre Universitaire, B.P. 34, 91898 Orsay Cedex, France

Received (in Cambridge, UK) 6th August 2002, Accepted 3rd September 2002

First published as an Advance Article on the web 19th September 2002

Large pore ( $a = 150\text{--}200\text{ \AA}$ ) wormlike and highly oriented cubic ( $Im\bar{3}m$  space group) and 2D-hexagonal ( $P6m$ ) mesostructured xerogels have been reproducibly synthesised by Evaporation-Induced Self Assembly (EISA). Mesostructure control was attained by changing the template (nonionic block copolymer) and water ( $h = [\text{H}_2\text{O}]/[\text{Si}]$ ) ratio.

The controlled synthesis of mesoporous materials by combining self-assembly of a supramolecular template and sol-gel chemistry is a subject that has seen explosive growth over the last decade.<sup>1,2</sup> Nonionic Amphiphilic Block Copolymer (ABC) templates have been widely applied to obtain large pore size and thick inorganic walls,<sup>3</sup> such as SBA-15 ( $P6m$ ) and SBA-16 ( $Im\bar{3}m$ ),<sup>3b</sup> or the FDU series.<sup>4</sup> All these methods give rise to mesostructured powders. Evaporation-Induced Self Assembly (EISA)<sup>5</sup> methods are interesting because they permit the control of the shape of the object (thin films,<sup>6</sup> xerogels,<sup>7</sup> aerosols<sup>8</sup>) as well as the mesostructure. Pluronic-templated  $P6m$  films have been completely characterised by TEM and 2D-SAXS.<sup>9</sup> Monoliths presenting  $P6m$  and a minor cubic mesophase have been exhaustively characterised.<sup>10</sup> Although EISA-based synthesis routes are very sensitive to solution and environment parameters, these effects are beginning to be understood.<sup>5-9,11</sup> Thus, the ability to tailor the mesostructure, shape, homogeneity and orientation of films or membranes by modifying these appropriate synthesis parameters (instead of a combinatorial approach) presents a major interest. In particular, three-dimensional ordered phases are interesting for membrane technology, ultra-low dielectric constant materials or coatings with enhanced mechanical properties.

In this work, we present a simple and reproducible EISA-based method to obtain large-pore ( $d_p > 60\text{ \AA}$ ) worm-like, cubic ( $Im\bar{3}m$ ) or 2D-hexagonal ( $P6m$ ) hybrid mesophases. The obtained phase can be easily tailored by varying the synthesis conditions, in particular, the template nature (P123 or F127) and the water contents ( $h = [\text{H}_2\text{O}]/[\text{Si}]$ ) in the initial sols.

Initial solutions were prepared by mixing a prehydrolysed silica sol† with an alcoholic solution of the template. The template:silica volume percentage ( $V_{\text{TS}\%}$ , estimated according to ref. 11c) was set between 25 and 60%. Subsequently, additional  $0.01\text{ mol dm}^{-3}$  HCl was added under vigorous stirring until homogenisation. Solutions were then aged in open flat-bottomed recipients, under quiescent conditions or air flux in controlled humidity (30–60% RH). The environment is critical, and the best organisation is obtained in a relatively humid atmosphere (RH > 45%) and low air flux. Self-standing films or flat xerogels (disks of ca.  $100\text{ }\mu\text{m}$  thickness, 2–3 cm diameter) are formed within 24 hours. Table 1 presents the synthesis conditions and resulting structures for a selection of the obtained mesophases. XRD patterns were taken at the D43 line of LURE (sample-detector distance of 620 mm;  $\lambda = 1.44\text{ \AA}$ ; integration time 20–40 min; image plate detectors). XRD patterns at incidence normal to the sample† (i.e. through the plane of the sample disk) give rise to diffraction rings, which are

Table 1 Synthesis conditions and sample characterisation

Sample	$h$	$s \times 10^3$	$V_{\text{TS}\%}$	Mesophase <sup>a</sup>	$a_{\text{XRD}}/\text{\AA}$
F-35-1	1	1.6	35	WL	163
F-35-3	3	1.6	35	H	184
F-35-5	5	1.6	35	C	183
F-50-5	5	3	50	C	187
P-50-5	5	3	50	H	206

<sup>a</sup> WL: Worm-like ( $a_{\text{XRD}} = d_{100}$ )—H 2D-hexagonal  $P6m$ —C cubic  $Im\bar{3}m$ .

characteristic of polyoriented domains. 2D-XRD patterns in near grazing incidence ( $\theta \sim 1\text{--}2^\circ$  with respect to the sample) for F127-templated silica (Fig. 1 a–c) show different mesostructures, according to the water content in solution. For  $h = 1$ , rings are obtained; this is typical of diffraction entities polyoriented in space (i.e., a worm-like structure, or randomly oriented channels<sup>12</sup>). For  $h \geq 3$ , well defined spots, as in oriented thin films or monoliths, are observed, suggesting that the hybrid mesophases are preferentially oriented. For  $h = 3$ , the  $d$ -spacing ratios ( $1:\sqrt{3}:2:\sqrt{7}$ ) and angles correspond to a  $P6m$  phase with channels aligned parallel to the sample flat surface.<sup>9,12</sup> The spots in samples of  $h > 3$  present ratios ( $1:\sqrt{2}:\sqrt{3}:\sqrt{4}:\sqrt{5}\dots$ ) and angles that correspond to a cubic phase that can be indexed as  $Im\bar{3}m$ ; (ESI†), as previously found in F127-templated silica thin films<sup>6</sup> and F127-ethanol-water media.<sup>13</sup> This is the first time that such an oriented cubic hybrid phase has been fully characterised by 2D-XRD, giving a total idea of the symmetry and orientation of the hybrid mesostructure. From the 2D-XRD information, the cubic mesostructures are oriented with a  $\{110\}$  plane parallel to the surface ( $c$ //film surface, Fig. 2d). According to the normal

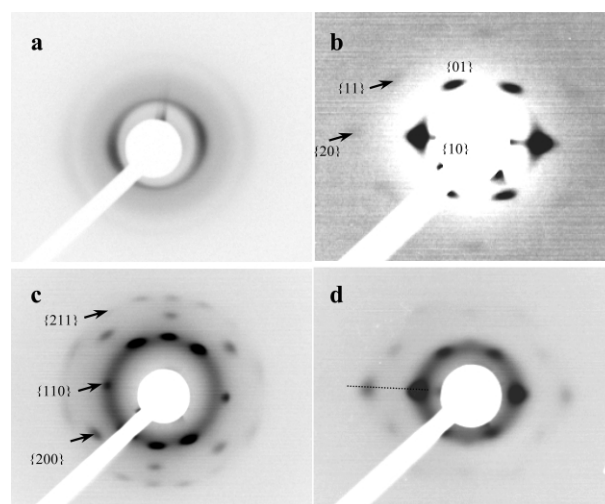


Fig. 1 2D-XRD patterns at an incidence of  $2^\circ$  of F127-templated self-standing films ( $s = [\text{surf}]/[\text{Si}] = 1.6 \times 10^{-3}$ ) with increasing water content. a)  $h = 1$ ; b)  $h = 3$ ; c)  $h = 5$ ; d) P123-templated film, with  $h = 5$ ,  $s = 5 \times 10^{-3}$ . The film was held in vertical position relative to these diagrams. The dotted line in d) shows the reciprocal space sampled by  $\theta$ - $2\theta$  XRD.

† Electronic supplementary information (ESI) available: TEM and indexation of cubic  $Im\bar{3}m$  hybrid mesophase, comparison of the synthesis conditions. See <http://www.rsc.org/suppdata/cc/b2/b207595d/>

incidence results, the *c* vector has little or no preferential orientation in the plane of the film surface,<sup>§</sup> in agreement with recent work by the Stucky group;<sup>11c</sup> however, in previously reported cubic thin films, a different orientation was proposed.<sup>6</sup> Interestingly, the (110) planes of the *Im3m* structure are the most densely packed in the lattice. The same effect (most dense planes preferentially oriented parallel to the sample surface) is observed for the *P6m* structures (Fig. 1b,d), and in thin films already reported.<sup>9,12</sup> Indeed, there is an epitaxial relationship between these two structures.<sup>14</sup> A fusion of micelles along the (1-11) direction of the *Im3m* cell leads to hexagonal channels, without changing the alignment of the cubic mesostructure.

TEM images of typical as-prepared and calcined (500 °C, 5 h, static air) cubic and hexagonal self-standing films or xerogels are presented in Fig. 2 a–c. Periodic distances are in agreement (within 15%) of those found by 2D-XRD (due to tilting or sample shrinkage under the electron beam). For the cubic F-35-5 treated at 135 °C, and 500 °C, *a* values of 159 and 121 Å are found respectively. In the case of hexagonal F50-3 treated at 135°, *a*<sub>TEM</sub> = 127 Å, which compares well with the XRD value, keeping in mind the contraction upon thermal treatment.

It is recognised that the choice of the template (P123 leads to *p6m* mesostructures) and *V*<sub>TS%</sub> are determinant in the final mesostructure.<sup>11a,c</sup> However, the results shown here demonstrate clearly that the water content in solution *h*, is a crucial variable. In these ‘silicatropic’ hybrids, the final mesostructure can be tailored by *h*, at a constant *V*<sub>TS%</sub>; indeed, hexagonal phases are obtained in conditions where cubic phases are expected (*V*<sub>TS%</sub> < 70%). It can be assumed that the water not consumed in silica hydrolysis–condensation is mostly placed at the silica–template hydrophilic hybrid interface (HI). In more water-rich systems, structures presenting higher curvature should be favoured.<sup>13,14</sup> That is, the mesostructure is not only directed by the volume fraction of the template, but also by the amount of the silica–template interface. The energetical contribution of the interface,  $\Delta G_{\text{interf}}$ , becomes important: more pores are formed, resulting in thinner walls. Addition of water helps to ‘fold’ the template in a more curved form, but also creating more hydrophilic silanol ends. A more ‘hydrophilic’ HI (water/ inorganic) will tend to maximise interactions with the template, and enhance curvature. The same effect has been observed in silica/CTAB films<sup>15</sup> and titania/template worm-like and hexagonal phases.<sup>11b,16</sup> It seems that this ‘modulation of the hydrophilic/hydrophobic character of the interface (MHHI)’

model can also be applied to silica. However, kinetic considerations (*i.e.*, evaporation *versus* the effects of condensation and gel viscosity<sup>11d</sup>) must be taken into account to give a complete picture of mesophase formation (ESI†).

In summary, we present an EISA-based simple and reproducible method that gives rise to a variety of mesostructures by changing a key parameter, the water:silica ratio (*h*). These mesostructures are analogues to the known MSU-X, SBA-15 or SBA-16; the cubic and hexagonal xerogels show a high degree of organisation and orientation, probably due to the organising effects of the air–gel and container–gel interfaces.<sup>7</sup> The experiments presented clearly demonstrate that water is a fundamental factor that can also control the obtained mesostructure by modulating the hydrophilic/hydrophobic character of the inorganic–template interface. Experiments are under way to completely describe and compare the formation paths of these mesophases, and the characteristics of the oxides that are obtained after calcination.

## Notes and references

‡ Prehydrolysed sols were prepared by heating a TEOS–HCl (0.1 mol dm<sup>−3</sup>)–ethanol mixture (*h* = [H<sub>2</sub>O]/[Si] = 1; *r* = [EtOH]/[Si] = 3) at 70 °C for 60 minutes. Synthesis solutions were prepared by mixing 2.5 g of this sol with the template. Samples were labelled X-*V*<sub>TS%</sub>-*h*; X = F or P (for Pluronic F127 or P123 templates respectively, see Table 1).

§ Depending on the orientation, *P6m* and *Im3m* 2D-XRD patterns are relatively similar, particularly if combined with uniaxial contraction. The key for a correct identification relies in the second order spots (as shown in Fig. 1, see also ESI), which are hard to detect, particularly in thin films, due to very low quantities of matter; this has often led to misinterpretation or erroneous indexing of the cubic phases.<sup>11c</sup>

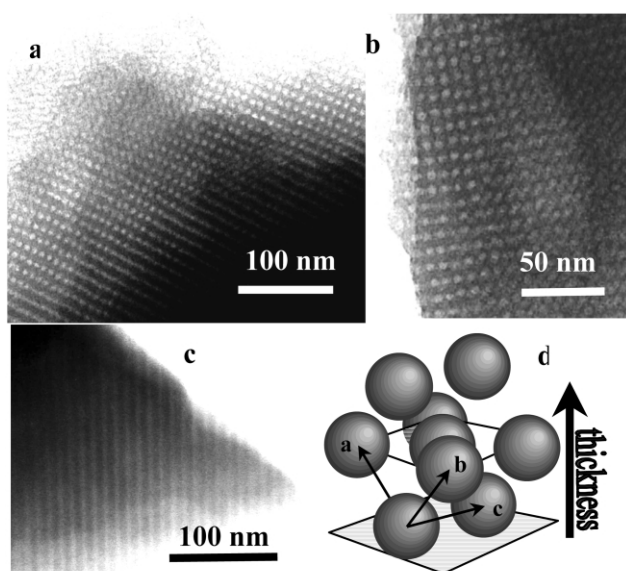


**Fig. 2** a,b) TEM images of *Im3m* mesostructured silica F-35-5; a) 135 °C, along [110]; b) calcined at 500 °C along [100]. c) Channels of a hexagonal F-35-3 hybrid. d) Orientation scheme for the cubic hybrids; mesopores are represented by the grey spheres.

- C. T. Kresge, M. E. Leonowicz, W. J. Roth, J. C. Vartuli and J. S. Beck, *Nature*, 1992, **359**, 710.
- (a) G. J. A. A. Soler-Illia, C. Sanchez, B. Lebeau and J. Patarin, *Chem. Rev.*, 2002, in press; (b) J. Y. Ying, C. P. Mehnert and M. S. Wong, *Angew. Chem., Int. Ed.*, 1999, **38**, 57.
- (a) P. T. Tanev, M. Chibwe and T. J. Pinnavaia, *Nature*, 1994, **368**, 321; (b) D. Zhao, Q. Huo, J. Feng, B. F. Chmelka and G. D. Stucky, *J. Am. Chem. Soc.*, 1998, **120**, 6024; (c) C. G. Goltner and M. Antonietti, *Adv. Mater.*, 1997, **9**, 431.
- C. Yu, Y. Yu, L. Miao and D. Zhao, *Microporous Mesoporous Mater.*, 2001, **44–45**, 65.
- C. J. Brinker, Y. Lu, A. Sellinger and H. Fan, *Adv. Mater.*, 1999, **11**, 579.
- D. Zhao, P. Yang, N. Melosh, J. Feng, B. F. Chmelka and G. D. Stucky, *Adv. Mater.*, 1998, **10**, 1380.
- (a) H. Yang, N. Coombs, Ö. Dag, I. Sokolov and G. A. Ozin, *J. Mater. Chem.*, 1997, **7**, 1755; (b) N. Yao, A. Y. Ku, N. Nakagawa, T. Lee, D. A. Saville and I. A. Aksay, *Chem. Mater.*, 2000, **12**, 1536.
- Y. Lu, R. Ganguli, C. A. Drewien, M. T. Anderson, C. J. Brinker, W. Gong, Y. Guo, H. Soye, B. Dunn, M. H. Huang and J. I. Zink, *Nature*, 1997, **389**, 364.
- D. Grosso, A. R. Balkenende, P. A. Albouy, A. Ayril, H. Amenitsch and F. Babonneau, *Chem. Mater.*, 2001, **13**, 1848.
- (a) N. A. Melosh, P. Davidson and B. F. Chmelka, *J. Am. Chem. Soc.*, 2000, **122**, 823; (b) N. A. Melosh, P. Lipic, F. A. Bates, F. Wudl, G. D. Stucky and B. F. Chmelka, *Macromolecules*, 1999, **32**, 4332.
- (a) M. Klotz, A. Ayril, C. Guizard and L. Cot, *J. Mater. Chem.*, 2000, **10**, 663; (b) G. J. A. A. Soler-Illia, A. Louis and C. Sanchez, *Chem. Mater.*, 2002, **14**, 750; (c) P. C. A. Alberius, K. L. Frindell, R. C. Hayward, E. J. Kramer, G. D. Stucky and B. F. Chmelka, *Chem. Mater.*, 2002, **14**, 3284; (d) G. J. A. A. Soler-Illia, D. Grosso, E. L. Crepaldi, F. Cagnol and C. Sanchez, *Mater. Res. Soc. Symp. Proc.*, 2002, **726**, paper Q7.3.
- (a) M. Klotz, P.-A. Albouy, A. Ayril, C. Ménager, D. Grosso, A. Van der Lee, V. Cabuil, F. Babonneau and C. Guizard, *Chem. Mater.*, 2000, **12**, 1721.
- R. Ivanova, P. Alexandridis and B. Lindmann, *Colloids Surf. A*, 2001, **183–185**, 41.
- P. Sakya, J. M. M. Seddon, R. H. Templer, R. J. Mirkin and G. J. T. Tiddy, *Langmuir*, 1997, **13**, 3706.
- F. Cagnol, D. Grosso, G. J. A. A. Soler-Illia, E. L. Crepaldi and C. Sanchez, *J. Mater. Chem.*, submitted.
- G. J. A. A. Soler-Illia, E. Scolan, A. Louis, P.-A. Albouy and C. Sanchez, *New J. Chem.*, 2001, **25**, 154.